Comparison of glow discharge cleaning and ionimpact desorption of stainless steel

D. N. Ruzic, G. A. Gerdin, and C. M. Loxton

Citation: J. Vac. Sci. Technol. A **4**, 1232 (1986); doi: 10.1116/1.573404

View online: http://dx.doi.org/10.1116/1.573404

View Table of Contents: http://avspublications.org/resource/1/JVTAD6/v4/i3

Published by the AVS: Science & Technology of Materials, Interfaces, and Processing

Related Articles

Enhanced electrical performance of Ag–Cu thin films after low temperature microwave processing
J. Vac. Sci. Technol. B 31, 011204 (2013)

Facile fabrication of scalable patterned nickel nanocone arrays for field emission applications
J. Vac. Sci. Technol. B 31, 02B104 (2013)

Nanostructuring of molybdenum and tungsten surfaces by low-energy helium ions
J. Vac. Sci. Technol. A 30, 041306 (2012)

Effects of the magnetic field strength on the modulated pulsed power magnetron sputtering of metallic films
J. Vac. Sci. Technol. A 29, 061301 (2011)

Scalability of plasma enhanced atomic layer deposited ruthenium films for interconnect applications
J. Vac. Sci. Technol. A 30, 01A103 (2012)

Additional information on J. Vac. Sci. Technol. A

Journal Homepage: http://avspublications.org/jvsta

Journal Information: http://avspublications.org/jvsta/about/about_the_journal

Top downloads: http://avspublications.org/jvsta/top_20_most_downloaded

Information for Authors: http://avspublications.org/jvsta/authors/information_for_contributors

ADVERTISEMENT

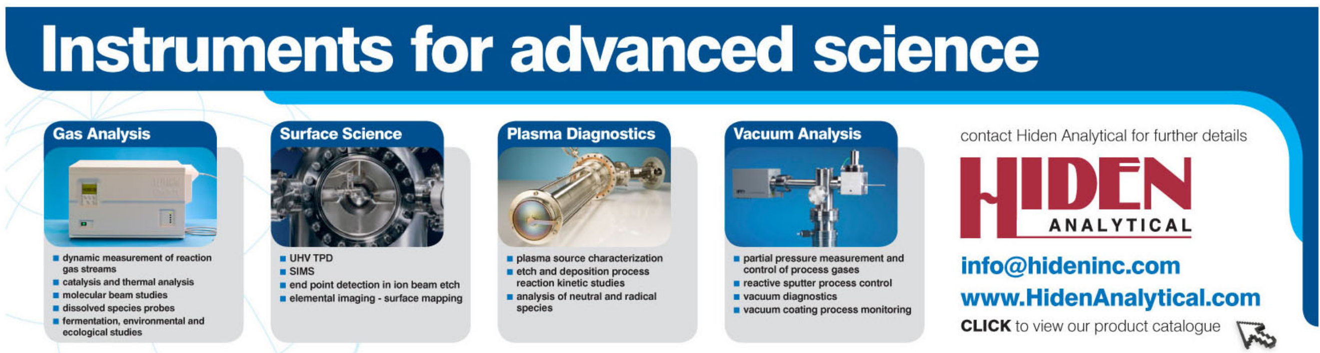

Downloaded 25 Dec 2012 to 130.126.32.13. Redistribution subject to AVS license or copyright; see http://avspublications.org/jvsta/about/rights_and_permissions

Comparison of glow discharge cleaning and ion-impact desorption of stainless steel

D. N. Ruzic and G. A. Gerdin
Nuclear Engineering Program, University of Illinois, Urbana, Illinois 61801

C. M. Loxton
Material Research Laboratory, University of Illinois, Urbana, Illinois 61801

(Received 7 October 1985; accepted 30 December 1985)

The effects of glow discharge cleaning (GDC) and ion-impact desorption (IID) of impurities on 302 stainless steel were compared using Auger electron spectroscopy (AES). Hydrogen GDC was done in a chamber attached to the Auger microprobe allowing transfer *in vacuo* to lessen recontamination. GDC removed the surface hydrocarbon layer, but deposited many constituents of the cathode and surrounding areas onto the sample. It also induced a high concentration of carbon which extended beyond the surface layer. The extent of the carbon layer varied with the prior treatment of the surface. IID is shown to maintain a higher surface purity. The feasibility of helium IID as an after-opening or between-shot cleaning technique for magnetic fusion experiments is discussed.

I. INTRODUCTION

The presence of adsorbed gas in magnetic fusion devices is problematic; it degrades plasma parameters.[1] Discharge cleaning is often used to alleviate this problem.[2] Thus the surfaces are subjected to neutral and ion bombardment. Though hydrogen GDC is accomplished primarily through chemical processes,[3] the bombardment also removes surface constituents under certain conditions. Contaminants, volatile compounds, and bulk material from the same and other regions of the discharge are redeposited[4] onto the very surface being cleaned. This recycling may be caused by ionization in the discharge,[5] and subsequent acceleration through the plasma sheath back toward the surface. The cleaning phase in fusion devices often lasts for weeks, wasting valuable machine time and discouraging future vacuum-vessel openings.

Another cleaning technique which subjects surfaces to ion bombardment is ion-impact desorption (IID) through the use of an energetic (1–3 keV) ion beam. Impurities are desorbed and some of the bulk surface material is sputtered. IID is extensively used prior to microsurface analysis and typically adds only the bombarding species onto the surface being cleaned. The desorbed and sputtered atoms form volatile compounds or are removed to less critical surfaces.

GDC and IID are also used extensively in substrate preparation and film deposition, and have been the subject of many investigations aimed at understanding or improving the production of semiconductor devices.[6–9] Plasma etching of silicon has been simulated by ion beams and studied *in situ* with an experimental setup similar to the one used here.[10,11]

To ascertain the usefulness of direct IID in cleaning magnetic fusion devices, the effects of both cleaning techniques need to be compared under controlled conditions. In this paper, atomic concentrations and depth profiles of the nonhydrogenic species near the surface of stainless steel samples cleaned by GDC versus IID methods are presented, surface removal rates are calculated, and geometrical limitations are discussed.

II. EXPERIMENTAL

Figure 1 shows a schematic of the apparatus. A simple sample-introduction/glow discharge chamber was attached to a Physical Electronics Model 545 scanning Auger microprobe so that a sample stage could be transferred, under vacuum, between the two chambers. The transfer rod was made with a Teflon insert to electrically isolate the 230 ± 10 cm^2, 240 ± 5 g aluminum sample stage from the chamber.

The samples mounted in positions 3 and 4 were 20 mil thick 1 cm $\times$ 1.5 cm 302 stainless steel. Two graphite samples were mounted in positions 1 and 2. All four samples were held in position by small copper clips. The stainless steel samples were cleaned prior to vacuum introduction following a standard cleaning procedure[12]: ethanol wipe, deionized water rinse, 15 min Alconox ultrasound, 15 min ultrasonic deionized water rinse, 1 h 125 °C bake.

IID was accomplished using a 1 keV argon or helium ion beam mounted in the Auger chamber. The beam was in-

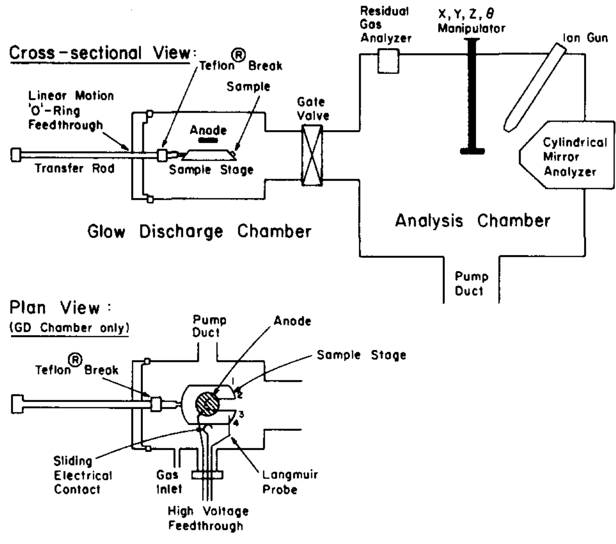

FIG. 1. Schematic of the apparatus. The numbers 1–4 refer to sample positions on the sample stage.

 0734-2101/86/031232-04$01.00 © 1986 American Vacuum Society

Downloaded 25 Dec 2012 to 130.126.32.13. Redistribution subject to AVS license or copyright; see http://avspublications.org/jvsta/about/rights_and_permissions

clined 42.5° with respect to the sample normal and had a current density of either 56.6, 52.0, or $35.6 \pm 0.5\ \mu A/cm^2$. All results shown have been normalized to the higher (56.6 $\mu A/cm^2$) current density. Auger analysis was performed in a vacuum of 10^{-9} Torr using a 3 keV electron beam and a peak-to-peak modulation voltage of 6 V.

For the GDC, the anode was a 20 mil thick, 4.5 cm diam stainless steel disk positioned 3 cm above the center of the sample stage. The cathode was the sample stage. It was connected to an electrical feedthrough by a stainless steel sliding contact. Two other feedthroughs were used as Langmuir probes. One was positioned about 1 cm above sample positions 3 and 4 (see Fig. 1), just above the plasma sheath. The other was about 3 cm from the side of the sample stage. The exposed probe tips were 0.2 ± 0.01 cm long, 20 mil diam tungsten wire. The sample stage and anode were biased independently with respect to the vacuum vessel (ground) by current limiting high voltage supplies. The samples were subjected to four hydrogen abnormal (cathode covered) glow discharges[13] lasting 30, 100, 20, and 35 min, respectively. The electron densities and temperatures were determined from Langmuir probe characteristics[14] and varied from 1 to $4 \times 10^8\ cm^{-3}$ and 2.2 to 4.5 eV. The pressure was 1.0 ± 0.05 Torr in the first and fourth discharge, but varied from 1 to 2.3 Torr in the middle discharges. A current density on the cathode of $290\ \mu A/cm^2$ was maintained in all the discharges. The cathode-fall potential V_c ranged from -250 to -310 V, the cathode-fall length L was 0.7 ± 0.2 cm, and the floating potential was close to 0 V.

Atomic concentrations were determined by dividing the peak heights by the Auger sensitivity.[15] This assumes a linear relationship which is strictly true only at low and moderate (30%) concentrations.[16] The atomic concentrations during the profiles were calibrated by using a least-squares fit to all the corresponding initial and final atomic concentrations. The errors in the atomic concentrations are on the order of 20% and arise from several sources: the uncertainty in the Auger peak heights, uncertainty in the sensitivity factors, uncertainty in the calibration of the profile data, and the differing escape depths of the Auger electrons.

Quantifying the depth of the profile is more difficult. A sputter rate of 16.8 ± 0.8 Å/min was determined for Ta_2O_5 by sputtering a 1000 Å Ta_2O_5 on Ta layer with the same 56.6 $\mu A/cm^2$, 1.0 keV Ar beam. Interpolation to the stainless steel samples used here requires knowledge of the relative sputtering yields for the particular incident beam energy and angle. Due to the uncertainties which this and altered layer effects[17] may introduce, the profiles were left in terms of sputtering time. The maximum depth resolution, set by the mean escape depth of the Auger electrons[16] for the elements of interest, is 6–8.5 Å.

III. RESULTS

Argon IID was primarily used in these experiments to speed data collection. It gave similar results to helium IID. Helium IID is recommended for fusion applications. IID by argon was used on a stainless steel sample after the standard cleaning procedure. The atomic concentrations and Auger depth profile are shown in Fig. 2(a). The shape of the initial

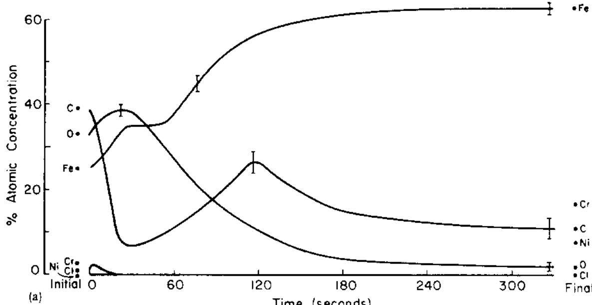

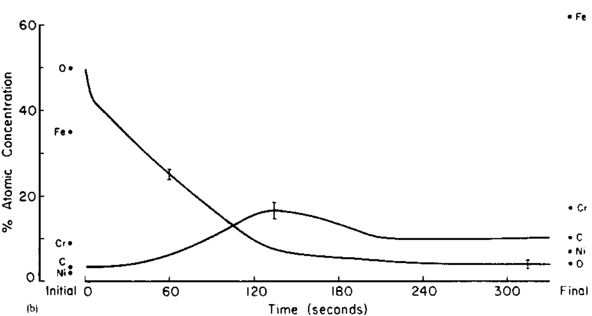

FIG. 2. Atomic concentration of 302 SS as a function of time during $56.6 \pm 0.5\ \mu A/cm^2$ 1000 eV Ar^+ bombardment: (a) after standard chemical cleaning procedure and (b) after 300 s of 1 keV Ar-ion bombardment followed by gas exposure.

carbon peak was indicative of hydrocarbon bonds, while the final shape was indicative of carbide bonds.[16] Auger analyses are consistent with the known bulk composition of the alloy, but indicate a much larger C concentration which can arise from several sources. This concentration is greatly enhanced by altered layer formation; in the steady state, the surface concentrations of the elements must be proportional to their bulk concentrations divided by their sputtering yields[18] and carbon has a low sputtering yield of 0.8 atoms/ion.[19,20] The C atomic concentration is also increased by segregation of C to the surface during prior treatment. Even the relatively low 125 °C temperature used in the prevacuum cleaning procedure is enough to enhance surface segregation of carbon in steel.[21] This effect has been well documented in other alloys.[22] Further, the removal rate (Å/min) will be lower where the concentration of C is the highest, effecting the depth resolution and shape of the C profiles.

In order to examine the possible contamination inherent in the vacuum transfer process, an already IID sputter-cleaned sample was transferred to the glow discharge chamber, exposed to 1 Torr of H_2, and returned. The resulting Auger profile is shown in Fig. 2(b). Some contamination, possibly resulting from CO and H_2O exposure is shown.

GDC in hydrogen was performed on two samples with different prior cleaning treatments. Analysis of a sample which underwent the standard cleaning procedure and was then H_2 GDC for the entire 185 min, is shown in Fig. 3(a). Although the surface C is reduced, Cu, Al, N, and S appear, indicating that redeposition from other surfaces has occurred. Some O contamination is also shown. The similarity to the results shown in Fig. 2(b) suggest this may result from

Downloaded 25 Dec 2012 to 130.126.32.13. Redistribution subject to AVS license or copyright; see http://avspublications.org/jvsta/about/rights_and_permissions

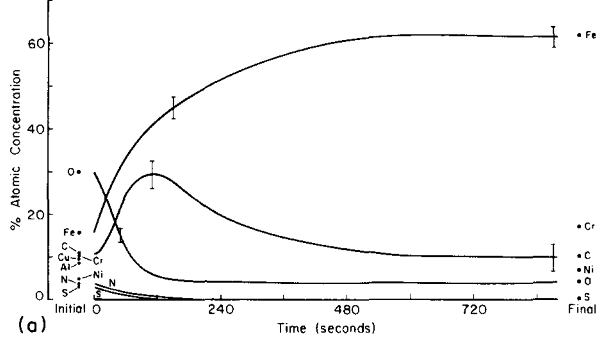

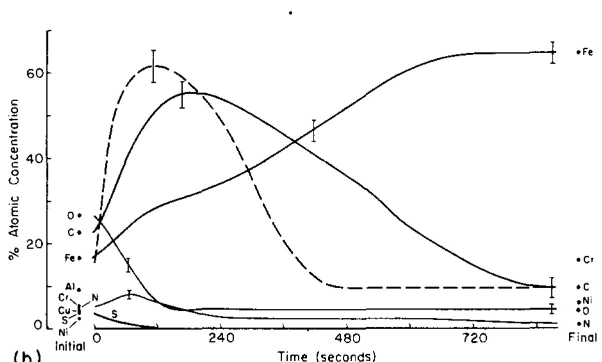

FIG. 3. Atomic concentration of 302 SS as a function of time during $56.6 \pm 0.5 \mu A/cm^2$ 1000 eV Ar^+ bombardment: (a) after 185 min of GDC and (b) after 300 s of 1 keV Ar-ion bombardment followed by 185 min of GDC. The dashed line is a C profile after the first 30 min of GDC.

the transfer process. The exponential removal of the O is consistent with surface desorption behavior.[23]

The other sample that underwent the standard cleaning procedure, was Ar ion beam cleaned from 300 s, and then H_2 GDC for 185 min. Atomic concentration and depth profile of this sample are shown in Fig. 3(b). The atomic concentrations and profiles differ significantly. There is much more C, and it occurs deeper than in the other sample [Fig. 3(a)]. There is also a N peak. The C profile obtained after the first 30 min of GDC is shown as a dashed line in Fig. 3(b). Even after this shorter period the C enhancement has developed.

Analysis of the residual gases in the glow discharge chamber indicated primarily H_2, with significant CO ($\sim 10\%$) and lesser amounts of CH_4, CH_3, CO_2, and H_2O, but little ($\sim 0.1\%$) O_2.

IV. DISCUSSION

During GDC, the samples and the entire cathode were subjected to energetic ion and neutral bombardment. (The walls of the chamber were not because of the independent biasing capabilities.) The energy distribution at the cathode[24] depends on the potential profile $V(z)$. For the discharge parameters used

$$V(z) = V_c[(2z/L) - (z^2/L)].$$

The ion current density calculated from this profile[13,25] depends most strongly on V_c and was consistent with the measured value of the ion current density. Mean energies of the ions and charge-exchange neutrals depends on L/l, where l is the mean-free-path of the neutrals. In abnormal glow discharges, L/l is independent of pressure[24] and for these discharge conditions equals 3.4. Also, in these types of discharges no full energy peak was observed.[24] Since the ions do not get the full potential energy eV_c mean ion and neutral energies can be used. These were calculated to be 0.4 V_c and 0.11 V_c, respectively, both with 65 mA currents.

This is a total flux of 3.6×10^{15} (atoms and ions)/cm^2 s (about twice the flux incident on the walls of the PLT tokamak near the limiter or during ICRF heating[26] but at about half of the energy). The removal rate caused by this flux is low. The sputtering coefficient for 115 eV H on Ni is only 0.0013 atoms/ion[27] and is similar for the other constituents. Thus the maximum removal rate from the GDC used here is approximately 0.33 Å/min. Particles are also being redeposited and embedded during this same period. From the depth of the observed N peak in Fig. 3(b), an implantation energy of 250 eV is predicted[20]—the same energy as the cathode fall. Note that the N peak is absent in Fig. 3(a)—the previously unsputtered sample. The presence of a hydrocarbon surface layer may protect the near-surface region from alteration.

The much higher C concentrations which occurred after GDC in the sputtered sample as compared to the unsputtered sample [Figs. 3(a) and 3(b)] could be due to the initial surface conditions. The initial surface layers of the two samples were quite different when GDC began. The difference in the N profiles also supports this protective surface layer explanation. Other possible explanations for the different C concentrations in Figs. 3(a) and 3(b) include more localized heating due to differences in energy reflection coefficients and/or the closer proximity of the previously sputtered sample (holder No. 3) to the C samples in holders 1 and 2. Another possible source of the C concentration is segregation induced by sample heating. Taking the particle and energy reflection coefficients into account,[28] 4.0 ± 0.2 W were incident on the sample stage. The primary cooling mechanism was radiation. Energy balance predicts a maximum temperature of 107 ± 3 °C after 100 min.

Surface removal rates can also be calculated for IID if the relative sputtering yields for Ta_2O_5 and stainless steel are known. Normal incidence sputtering yields were calculated[7,19] to be 2.7 atoms/ion for stainless steel and 2.5 atoms/ion for Ta_2O_5 using tabulated values[20] and a binding energy for stainless steel of 4.12 eV.[29] Neither of these yields were corrected for altered layer effects[17] which should reduce the sputtering yields, or nonnormal-incidence sputtering effects[30] which should increase the sputtering yields. The measured sputtering yield of Ta_2O_5 was 1.62 ± 0.08 atoms/ion. The same yield is adopted for stainless steel. Ar IID then gives the same removal rate, approximately 17 Å/min. The depth profiles using He were very similar in shape to those using Ar, but the He sputtering rate was 4.6 ± 0.6 times slower than with Ar, giving a removal rate of approximately 3.6 Å/min for the He IID used in this experiment. This is an order of magnitude higher than the GDC used in this experiment, but removal rates depend upon the current. The effective sputtering yield of He IID is three orders of magnitude higher than the GDC used in this experiment, though only small areas are affected by IID at any one time.

Downloaded 25 Dec 2012 to 130.126.32.13. Redistribution subject to AVS license or copyright; see http://avspublications.org/jvsta/about/rights_and_permissions

V. CONCLUSIONS

A combination of IID and then GDC leads to a significant enhancement of C near the surface compared to either GDC or IID alone. Both IID and GDC remove or reduce hydrocarbons and other adsorbates on the surface. However, GDC can result in significant uncontrolled redeposition from other exposed surfaces. In magnetic fusion applications, this could slow cleaning, and could lead to high-Z material being depositied in undesirable locations. IID, even with helium (at 1 keV), has a higher sputtering rate than the relatively high pressure GDC used in this experiment. For some applications with amenable geometry, such as the coaxial cylinders of a gun-type spheromak, divertor plates, and limiters, helium IID may lead to faster and more thorough cleaning. Based on the removal rates calculated in this paper, IID utilizing broad-beam (10–30 cm^2) high-current-density (1–3 mA/cm^2) He-ion sources[31–33] would remove contaminants from surface areas less than 4000 cm^2 at least ten times faster than the GDC studied in this experiment.

ACKNOWLEDGMENTS

This work made use of facilities in the Center for Microanalysis of Materials of the University of Illinois Materials Research Laboratory. One of the authors (C.M.L) acknowledges support by the U.S. Department of Energy under Contract No. DE-AC02-76ER01198.

[1]R. Behrisch and B. B. Kadomtsev, in *Proceedings of the 5th International Conference in Tokyo*, 1974 (IAEA, Vienna II, 1975), p. 229.
[2]G. M. McCracken and P. E. Stott, Nucl. Fusion **19**, 889 (1979).
[3]H. F. Dylla, J. Nucl. Mater. **93 & 94**, 61 (1980).
[4]H. F. Dylla, K. Bol, S. A. Cohen, R. J. Hawryluk, E. B. Meservey, and S. M. Rossnagel, J. Vac. Sci. Technol. **16**, 752 (1979).
[5]D. Ruzic, S. Cohen, B. Denne, and J. Schivell, J. Vac. Sci. Technol. A **1**, 818 (1983).
[6]J. L. Vossen, J. Phys. E **12**, 159 (1979).
[7]J. E. Greene, CRC Crit. Rev. Solid State Mater. Sci. **11**, 47 (1982).
[8]J. L. Vossen, J. H. Thomas III, J.-S. Maa, and J. J. O'Neill, J. Vac. Sci. Technol. A **2**, 212 (1984).
[9]J. E. Houston and R. D. Bland, J. Appl. Phys. **44**, 2504 (1973).
[10]T. M. Mayer and R. A. Barker, J. Vac. Sci. Technol. **21**, 757 (1982).
[11]J. L. Vossen, J. H. Thomas III, J.-S. Maa, O. R. Mesker, and G. O. Fowler, J. Vac. Sci. Technol. A **1**, 1452 (1983).
[12]Princeton Plasma Physics Laboratory's Vacuum Preparation Lab (personal communication, July, 1985).
[13]S. C. Brown, *Basic Data of Plasma Physics* (MIT and Wiley, New York, 1959), p. 275.
[14]G. J. Schulz and S. C. Brown, Phys. Rev. **98**, 1642 (1955).
[15]L. E. Davis, N. C. MacDonald, P. W. Palmberg, G. E. Riach, and R. E. Webar, *Handbook of Auger Spectroscopy* (Physical Electronics Industries, Eden Prairie, MN, 1976).
[16]J. C. Riviere, Contemp. Phys. **14**, 513 (1973).
[17]E. Taglauer and W. Heiland, Appl. Phys. Lett. **33**, 950 (1978).
[18]J. W. Coburn, Thin Solid Films **64**, 371 (1979).
[19]P. Sigmund, Phys. Rev. **184**, 383 (1969).
[20]K. B. Winterbon, *Ion Implantation Range and Energy Deposition Distributions* (IFI/Plenum, New York, 1975), Vol. 2.
[21]C. L. Briant and S. K. Banerji, Int. Met. Rev. No. **4**, 164 (1978).
[22]J. J. Burton, B. J. Berkowitz, and R. D. Kane, Metall. Trans. A **10A**, 677 (1979).
[23]W. Heiland and E. Taglauer, Inst. Phys. Conf. Ser. No. **38**, 287 (1978).
[24]W. D. Davis and T. A. Vanderslice, Phys. Rev. **131**, 219 (1963).
[25]S. C. Brown, *Basic Data for Plasma Physics* (MIT, Cambridge, 1967).
[26]S. A. Cohen, D. N. Ruzic, D. E. Voss, R. Budny, P. Colestock, D. Heifetz, J. Hosea, D. Hwang, D. Manos, and J. Wilson, Nucl. Fusion **24**, 1490 (1984).
[27]J. Bohdansky, Nucl. Fusion (special issue) **1984**, 61.
[28]W. Eckstein, Nucl. Fusion (special issue) **1984**, 12.
[29]O. Kubaschewski, E. L. L. Evans, and C. B. Alcock, *Metallurgical Thermochemistry* (Pergamon, New York, 1967).
[30]H. Oechsner, Z. Phys. **261**, 37 (1973).
[31]H. R. Kaufman, J. J. Cuomo, and J. M. E. Harper, J. Vac. Sci. Technol. **21**, 725 (1982).
[32]J. M. E. Harper, J. J. Cuomo, and H. R. Kaufman, J. Vac. Sci. Technol. **21**, 737 (1982).
[33]H. R. Kaufman, J. M. E. Harper, and J. J. Cuomo, J. Vac. Sci. Technol. **21**, 764 (1982).

Downloaded 25 Dec 2012 to 130.126.32.13. Redistribution subject to AVS license or copyright; see http://avspublications.org/jvsta/about/rights_and_permissions